

³¹P saturation transfer and phosphocreatine imaging in the monkey brain

(³¹P NMR imaging/creatinase/visual stimulation)

BASSEM MORA*[†], P. T. NARASIMHAN*[‡], BRIAN D. ROSS*[‡], JOHN ALLMAN[†], AND PETER B. BARKER*[§]

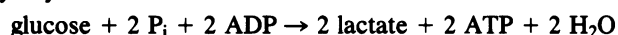
*Huntington Medical Research Institutes, 660 South Fair Oaks Avenue, Pasadena, CA 91105; and [†]Divisions of Biology and [‡]Chemistry and Chemical Engineering, California Institute of Technology, Pasadena, CA 91125

Communicated by John D. Roberts, May 15, 1991

ABSTRACT ³¹P magnetic resonance imaging with chemical-shift discrimination by selective excitation has been employed to determine the phosphocreatine (PCr) distribution in the brains of three juvenile macaque monkeys. PCr images were also obtained while saturating the resonance of the γ -phosphate of ATP, which allowed the investigation of the chemical exchange between PCr and the γ -phosphate of ATP catalyzed by creatine kinase. Superposition of the PCr images over the proton image of the same monkey brain revealed topological variations in the distribution of PCr and creatine kinase activity. PCr images were also obtained with and without visual stimulation. In two out of four experiments, an apparently localized decrease in PCr concentration was noted in visual cortex upon visual stimulation. This result is interpreted in terms of a possible role for the local ADP concentration in stimulating the accompanying metabolic response.

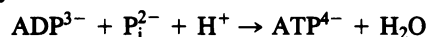
As part of a study to map the biochemical correlates of neural activity in the primary and associated visual areas of the primate cortex, we have undertaken ³¹P magnetic resonance (MR) studies of the macaque monkey brain. In this species, as in man, visual stimulation may be expected to involve the following three principal reactions for metabolic energy production within the primary visual cortex, where PCr is phosphocreatine, Cr is creatine, and CK is creatine kinase.

Glycolysis:



CK reaction: $\text{PCr}^{2-} + \text{ADP}^- + \text{H}^+ \rightarrow \text{Cr} + \text{ATP}^{2-}$

Oxidative phosphorylation:



Positron emission tomography (PET) studies on humans have shown that with visual stimulation blood flow and glucose consumption are increased (1–3). Localized proton MR studies have revealed a short-term increase in lactate concentration in the human brain upon visual stimulation (4). Thus it may be surmised from both PET and MR studies that glycolysis is important in visual stimulation. The local increase in cerebral oxygen consumption (mean = 5%, as measured by PET) due to somatosensory stimulation is less than the corresponding local increase in cerebral blood flow (mean = 29%) (5). Despite the small increase in the oxygen consumption noted in these PET studies, there appears to be a role for oxidative phosphorylation, although it seems from these studies that over longer times the role of the glycolysis reaction is significant. The role of the CK reaction is in provision and transport of ATP, but the question whether visual stimulation

results in any increase in CK activity has not yet been addressed by these PET studies or by MR techniques.

A further point is the interaction of these three pathways of putative energy synthesis. An intermediate common to all three pathways is ADP. The local concentration of free ADP may determine flux through oxidative phosphorylation (6); it may also influence flux through glycolysis at one or more sites but, particularly indirectly, through allosteric effects of ATP or AMP on phosphofructokinase (7). The concentration of ADP is in turn determined by equilibrium reactions, among which CK is most significant (8). We may, therefore, expect to obtain useful information about all three reactions by observation of PCr concentration and determination of the equilibrium of CK, from which ADP concentration can be calculated.

The great heterogeneity of cerebral circulation and metabolism observed in PET studies leaves room for doubt about MR assays, which are only performed at a single time point and confined to the anticipated region of interest. To assess the response of the CK reaction to visual stimulation, it would be helpful to monitor PCr levels and CK flux in several areas of the primate brain simultaneously and repeatedly.

MR spectroscopic imaging has been used to visualize changes in metabolite concentration and flux *in vivo* (9–21). Based on the magnetization-transfer technique (22), it is also possible to saturate the γ -phosphate of ATP (γ -ATP) signal and observe the reduction in the intensity of the PCr signal and vice versa (23). The magnetization transfer thus observed is a measure of CK flux in the forward and reverse directions, respectively (for reviews, see refs. 24 and 25).

Hsieh and Balaban (26) obtained PCr images of the rabbit leg skeletal muscle using a Hahn spin-echo pulse sequence. In monkey brain, spin-echo spectra showed noticeable presence of the γ -ATP signal in addition to the PCr signal. We have, therefore, employed selective excitation and a phase- and frequency-encode ³¹P spin-echo imaging procedure to obtain pure PCr images.

In the present work, we obtained ³¹P images of the PCr distribution in the monkey brain with and without saturation of the γ -ATP resonance. Such images provide a measure of the distribution of CK. This presents the possibility of observing noninvasively by MR imaging techniques any alteration in PCr levels or CK activity due to visual stimulation.

METHODS

Animal Preparation. The monkey used in this study was a juvenile female macaque (weight, 1.6 kg) belonging to the species *Macaca fascicularis*. Animal handling procedures

Abbreviations: PCr, phosphocreatine; CK, creatine kinase; PET, positron emission tomography; MR, magnetic resonance; TE, echo time; TR, repetition time; γ -ATP, γ -phosphate of ATP.

[§]Present address: Division of NMR Research, Johns Hopkins Hospital, 600 North Wolfe Street, Baltimore, MD 21205.

The publication costs of this article were defrayed in part by page charge payment. This article must therefore be hereby marked "advertisement" in accordance with 18 U.S.C. §1734 solely to indicate this fact.

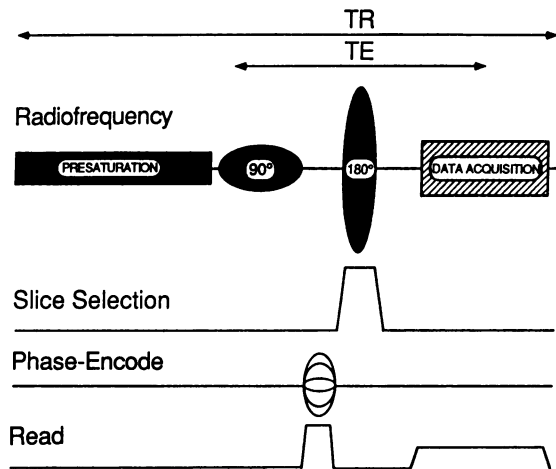


FIG. 1. Pulse sequence used to obtain the PCr images. A sinc 90° pulse is followed by phase-encode and dephasing-observe gradients, followed by a slice-selective 180° pulse and then data acquisition in the presence of a frequency-encoding readout gradient. For the saturation-transfer images, the saturating irradiation was present during the period labeled presaturation in the figure. The frequency of this irradiation was either that of γ -ATP at -2.5 ppm from PCr or at the control position at $+2.5$ ppm from PCr.

followed were those approved by Committees on Animal Care and Use at the California Institute of Technology and the Huntington Medical Research Institutes. Anesthesia was maintained by repeated intramuscular injections of ketamine. The stability of the biological sample was tested by acquiring fully relaxed whole-volume ^{31}P spectra at regular intervals over the 10-hr experimental session.

Visual Stimulation. A stroboscopic light source with a variable flicker rate was employed. Visual stimulation was applied for 30-min periods interleaved with 30 min of control (no stimulus). During the visual stimulation period, the light source flicker rate was altered every 3 min to minimize the effects of habituation. The rate was varied from 8 Hz to 4 Hz and 12 Hz. Related PET studies have revealed a maximum response in the visual cortex of humans to a flicker rate of 8–10 Hz (1).

Imaging Procedures. ^{31}P data were obtained at 81.01 MHz using a General Electric CSI-II spectrometer interfaced to an Oxford Research System 4.7-T magnet. A one-turn solenoidal coil (diameter, 9 cm; length, 6.5 cm) tunable to ^1H and ^{31}P was used.

A spin-echo proton image was first acquired with an echo time (TE) of 30 msec and a repetition time (TR) of 2 sec. The ^{31}P imaging sequence (Fig. 1) consisted of a frequency-selective non-slice-selective phase-cycled one-lobe 90° sinc pulse of 10-msec duration set on the PCr resonance so as to selectively excite this peak with a bandwidth of less than 200 Hz. In the saturation-transfer experiments, a TE of 28 msec, a TR of 4 sec, and 100 scans per phase-encode step were employed. In the visual stimulation experiments, a slice thickness of 20 mm and 24 scans per phase-encode step were used.

For the saturation-transfer studies, a second irradiation frequency was centered at $+2.5$ ppm (PCr = 0 ppm), whereas for the saturated image it was centered at -2.5 ppm, the frequency of γ -ATP. A modified partial k -space acquisition scheme (27) was used, in which only the middle 16 phase-encode steps were acquired out of a possible maximum of 32 steps. Tests on a ^{31}P phantom showed no significant loss of image quality or intensity due to zero filling. The 32×32 pixel PCr images were subsequently linearly interpolated along the horizontal and vertical dimensions to produce images corresponding in size to the proton images.

In the visual-stimulation studies, PCr images were acquired without a second saturating irradiation at 30-min intervals with visual stimulation during alternate 30-min periods. The control and visual-stimulus 30-min raw data files were added to yield the final images. Difference images were obtained by subtracting the stimulus from the control images.

RESULTS

Fig. 2 C and D illustrates the selective excitation of PCr achieved using sinc pulses in the spin-echo sequence. The fully relaxed ^{31}P spectrum is shown in Fig. 2A, acquired with a 90° pulse width, a predelay of 16 sec, a spectral width of 5000 Hz, and 32 averages; the broad brain hump was removed by convolution difference processing followed by minor baseline adjustments. The elimination in Fig. 2C of the peaks

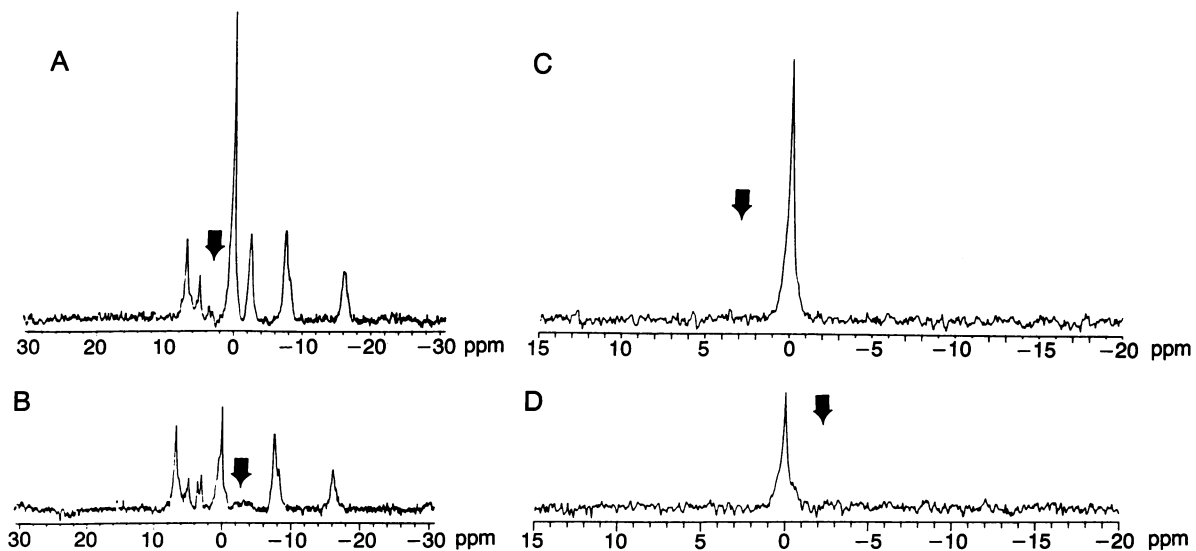


FIG. 2. (A) Whole-brain "pulse-and-collect" ^{31}P spectrum acquired with control irradiation from a second transmitter centered at $+2.5$ ppm from PCr resonance. (B) Spectrum with γ -ATP irradiation. (C) Whole-brain spin-echo spectra with control irradiation at $+2.5$ ppm from a PCr resonance. (D) Spectrum with γ -ATP irradiation. Acquisition parameters are as follows: TR, 6 sec; TE, 30 msec; a 90° one-lobe sinc pulse; a one-lobe 3-msec 180° pulse; 32 excitations. Saturating irradiation was present throughout the predelay period, and its location is shown by the arrows.

seen in Fig. 2A was accomplished by a spin echo and reduction in the excitation band width from 5000 Hz to <200 Hz. Sinc pulse parameters optimized in this manner with ^{31}P MR spectroscopy were then used for imaging. The effect of saturating $\gamma\text{-ATP}$ is demonstrated in Fig. 2A and B, where the irradiation is centered at +2.5 ppm (control) and -2.5 ppm (on $\gamma\text{-ATP}$), respectively. The degree of saturation achieved was noted in Fig. 2B, and transfer of magnetization to PCr was identical for selective excitation (Fig. 2D). Fig. 2C shows the selectively excited PCr resonance with a second control irradiation at +2.5 ppm and Fig. 2D shows this resonance with the irradiation centered on the $\gamma\text{-ATP}$ resonance at -2.5 ppm. The decrease in intensity of the PCr resonance is attributed to the magnetization transfer between $\gamma\text{-ATP}$ and PCr, due to a chemical exchange catalyzed by CK. Transfer of magnetization was $67 \pm 4\%$ ($n = 5$; i.e., $M_s/M_o \approx 0.33 \pm 0.02$, where M_o is the control PCr magnetization and M_s is the magnetization of PCr when the $\gamma\text{-ATP}$ signal is saturated), a value in complete agreement with the previously recorded CK activity in mammalian brain. From these results, we calculate that flux through CK in monkey brain is close to $150 \mu\text{mol}\cdot\text{min}^{-1}\cdot\text{g}^{-1}$, assuming ATP at $\approx 3 \text{ mM}$ and a PCr/ATP ratio of 2.7. The derivation of these values from both saturation-transfer and inversion-transfer studies is described in detail elsewhere (28).

Experiments with a phantom containing a 5 mM P_i solution yielded poor 30-min images due to the low signal-to-noise ratio, whereas experiments with a 10 mM P_i solution gave more uniform images of acceptable quality. From fully relaxed ^{31}P spectra of the monkey brain, we have obtained a

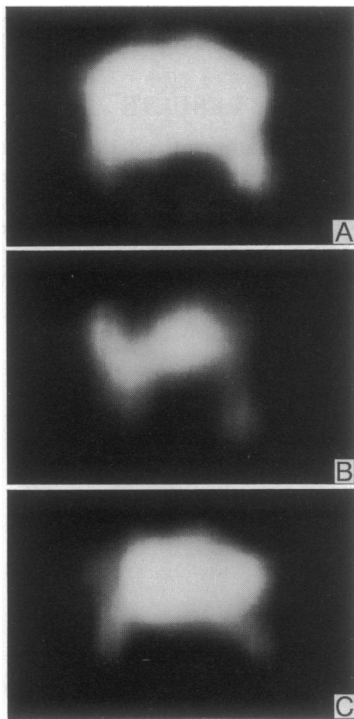


FIG. 3. Projection images of the spatial distribution of PCr in the monkey brain. Acquisition parameters are as follows: TR, 4 sec; TE, 28 msec; field of view, 160.25 mm; 100 excitations. The images correspond to projection images across the entire mediolateral axis of the brain as no slice selection was used. Partial k -space acquisition was used prior to Fourier transformation, and linear interpolation was employed to yield the final images. (A) PCr image obtained with control irradiation at +2.5 ppm from PCr. (B) PCr image obtained with $\gamma\text{-ATP}$ irradiation at -2.5 ppm from PCr. Both are displayed on the same intensity scale. The drop in signal intensity is due to the magnetization transfer between PCr and $\gamma\text{-ATP}$. (C) PCr difference image, obtained by subtracting B from A.

ratio of PCr/ $\gamma\text{-ATP}$ of 2.7. By using a $\gamma\text{-ATP}$ concentration of 3 mM (8, 29), the concentration of PCr in the monkey brain is estimated to be $\approx 8 \text{ mM}$. The PCr images of *in vivo* monkey brain, corresponding to the spectra discussed above (Fig. 2C and D), are shown in Fig. 3A and B, acquired in the midsagittal plane with eyes anterior and caput to the right. The intensity was sufficient to generate meaningful PCr images. Fig. 3A shows the PCr image obtained during control irradiation at +2.5 ppm and Fig. 3B shows the image obtained with irradiation on $\gamma\text{-ATP}$ at -2.5 ppm. A marked reduction in the intensity of the image is noticeable. The difference in image intensity during saturation of $\gamma\text{-ATP}$ was >50%, corresponding to the $\approx 67\%$ magnetization transfer to PCr seen during spectroscopy and expected from the rate of the CK reaction. The PCr images represent projection images across the entire mediolateral axis of the brain. The time required to obtain these PCr images was $\approx 1.8 \text{ hr}$ per image. The difference image, shown in Fig. 3C, conforms to the approximately uniform rate of CK activity across the entire volume of brain imaged in this study.

Fig. 4 shows the results of a visual stimulation experiment. Fig. 4A and B shows PCr images of a 20-mm midsagittal slice, with an in-plane resolution of $5 \text{ mm} \times 5 \text{ mm}$, yielding a voxel size of 0.5 cm^3 . The imaging time was 3.5 hr per image, and the k -space data file corresponded to the sum of 7 30-min data files. This sum was then Fourier-transformed and linearly interpolated to produce the final image. Fig. 4A is the control image and Fig. 4B is the image with visual stimulation. Fig. 4C is the corresponding midsagittal proton image, with a slice thickness of 5 mm and an acquisition time of $\approx 15 \text{ min}$. Some modest decrease in PCr intensity may be observed upon visual stimulation. This is more readily noted in difference images obtained by subtracting PCr images obtained during

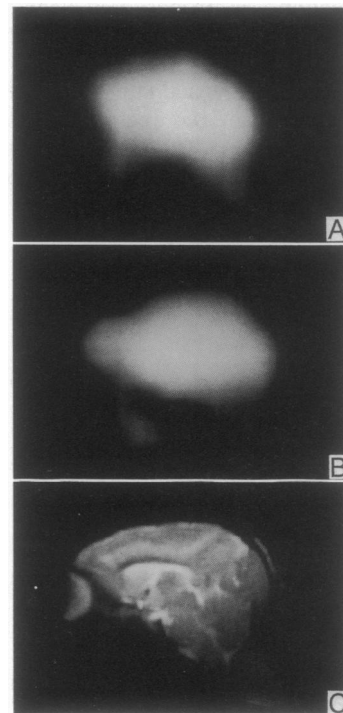


FIG. 4. PCr images of the monkey brain acquired without visual stimulation (A) and with visual stimulation (B). The images correspond to a slice thickness of 20 mm and have an in-plane spatial resolution of $5 \text{ mm} \times 5 \text{ mm}$. A TR of 4 sec, TE of 28 msec, partial k -space acquisition, and 24 excitations were used for each 30-min file acquired. These were subsequently added and then the final sum was Fourier-transformed and linearly interpolated. (C) Proton image corresponding to the PCr images acquired with a TR of 2 sec, a TE of 30 msec, and two acquisitions.

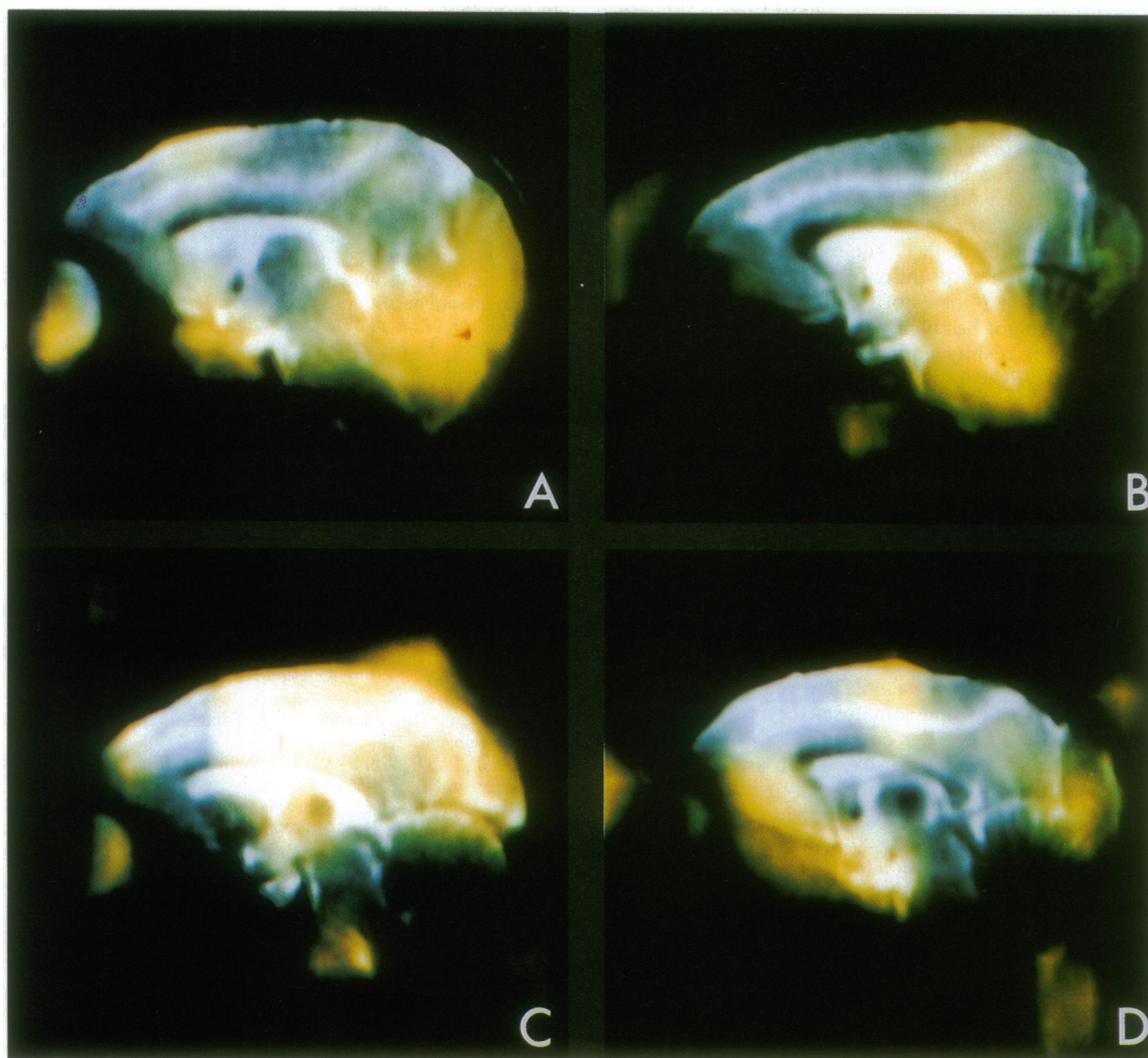


FIG. 5. Difference PCr images superimposed over the corresponding proton images from four experiments involving visual stimulation. The difference images were obtained by subtracting the visual stimulation image from the control image (no stimulus). Images in *A* and *B* correspond to the same monkey, whereas images in *C* and *D* are from two other monkeys. See text for discussion of the cortical areas being activated by the stimulus.

visual stimulation from those during dark periods. The resulting difference image of Fig. 4 *A* and *B* overlaid on the corresponding proton image (Fig. 4*C*) is shown in Fig. 5*A*. A region in the occipital cortex, possibly conforming to the primary visual cortex, appears to become relatively depleted of PCr during visual stimulation in this experiment. Fig. 5 *B*, *C*, and *D* shows difference images obtained from three other experimental sessions. The yellow overlay in these figures corresponds to regions of reduced PCr. The same monkey was used as in Fig. 5 *A* and *B*, whereas Fig. 5 *C* and *D* corresponds to two other animals. In Fig. 5*B*, the imaging time was 5.5 hr per image; in Fig. 5*C*, it was 2 hr; and in Fig. 5*D*, it was 5 hr (corresponding to eleven, four, and ten 30-min images, respectively). In each case some differences are to be found, but the area of brain most readily seen to be depleted of PCr was somewhat variable, so that we cannot clearly demonstrate the response within known visual cortex.

DISCUSSION

The difference image (Fig. 3*C*) represents the distribution in the monkey brain of the difference between the control PCr

magnetization (M_o) and the magnetization (M_s) of PCr when the γ -ATP signal is saturated. From the saturation-transfer equation (for example, see ref. 25), it can be seen that

$$(M_o - M_s) = M_o k_f (T_{1app}) = M_o k_f \{T_1 / (1 + k_f T_1)\},$$

where T_{1app} is the apparent spin-lattice relaxation time of PCr in the presence of a saturating irradiation set on the γ -ATP resonance. If the regional variations in T_1 are negligible, then this difference image can be correlated to the concentration of PCr through M_o and the forward rate constant k_f and, hence, to the CK activity in various regions of the brain. The quantity $M_o k_f$ is proportional to the forward flux of the CK reaction. In a separate study (28), we have determined the kinetic and relaxation parameters for the CK reaction in the living monkey brain. In particular, the value of k_f is 0.32 ± 0.02 sec and the value of T_{1app} for PCr is 2.13 ± 0.17 sec from saturation-transfer experiments and the value of T_1 for PCr is 5.54 ± 0.95 sec from inversion-transfer experiments. Thus $M_o - M_s$ corresponds to $0.62 M_o$, typically.

The images presented in Fig. 3 show increased signal in the center of the image due to the fact that these are projection

images across the entire thickness of the brain. The PCr image arising from a slice 20 mm thick displayed in Fig. 4A shows a better correlation with the anatomical image shown in Fig. 4C. A comparison of these two images clearly shows that the PCr signals arise from within the brain of the monkey and that there is negligible contribution from cranial muscle. The in-plane resolution in Fig. 4A and B is 5 mm × 5 mm, thereby producing a voxel volume of 0.5 cm³. The spatial variation in PCr levels shows that different areas of the brain maintain various stores of PCr. The exact reason for this is at present unclear. The present experiments do not rule out regional variations in T₁ or T₂ of PCr, or both. An effect of anesthesia also cannot be ruled out.

Our preliminary results concerning the effect of visual stimulation on the PCr distribution in the monkey brain are as follows: In two out of four experiments, there was a reduction in the PCr concentration localized to visual cortex with visual stimulation. The difference images (Fig. 5) show the cortical areas corresponding to these reductions. In Fig. 5A, the area of decreased PCr is located around the calcarine fissure in primary visual cortex and dorsal cerebellum. In Fig. 5B, the decreased PCr is centered in the brain stem and posterior thalamus, which contain the optic tectum and the lateral geniculate nucleus, the principal thalamic relay to visual cortex, but there is little reduction in cortex. In Fig. 5C, from a second monkey, the decreased PCr is located in the dorsal primary cortical visual area and extends into dorsal extrastriate visual cortex and somatosensory cortex. In Fig. 5D, from a third monkey, the decrease is located in orbitofrontal and somatosensory cortex, which are outside the visual system. In Fig. 5D, the poor signal-to-noise ratio has resulted in the difference signal falling outside the brain area.

The localized reduction in PCr concentration upon visual stimulation can be equated with a localized increase in ADP concentration. ADP is known to be an effective stimulator of oxidative phosphorylation (6) and would explain the increased oxygen consumption observed by PET studies, but ADP may also indirectly accelerate phosphofructokinase (30), and hence glycolysis, leading to the observed increase in lactate upon visual stimulation.

We thank Dr. V. Rajanayagam of Huntington Medical Research Institutes for help in processing the images. B.M. thanks Dr. Lloyd Smith of the University of California, San Francisco, for his encouragement. This work was supported by grants from the Magnetic Resonance Spectroscopy fund of the Huntington Medical Research Institutes, The L. K. Whittier Foundation of California, and The Norris Foundation, and by grants to J.A. from the Beckman Institute and Karl Kirchgessner Foundation.

1. Fox, P. T. & Raichle, M. E. (1984) *J. Neurophysiol.* **51**, 1109–1120.
2. Fox, P. T., Mintun, M. A., Raichle, M. E., Miezin, F. M., Allman, J. M. & Van Essen, D. C. (1986) *Nature (London)* **323**, 806–809.
3. Kushner, M. J., Rosenquist, A., Alavi, A., Rosen, M., Dan, R., Fazekas, F., Bosley, T., Greenberg, J. & Reivich, M. (1988) *Neurology* **38**, 89–95.
4. Prichard, J., Rothman, D., Novotny, E., Petroff, O., Avison, M., Howseman, A., Hanstock, C. & Shulman, R. G. (1989) *Soc. Magn. Reson. Med. Works-in-Prog.*, 8th Annual Meeting (Society of Magnetic Resonance in Medicine, Berkeley, CA), p. 1071 (abstr.).
5. Fox, P. T. & Raichle, M. E. (1986) *Proc. Natl. Acad. Sci. USA* **83**, 1140–1144.
6. Chance, B. & Williams, G. R. (1956) *Adv. Enzymol.* **17**, 65–80.
7. Newsholme, E. A. & Leech, A. R., eds. (1983) *Biochemistry for the Medical Sciences* (Wiley, New York).
8. Veech, R. L., Lawson, J. W. R., Cornell, N. W. & Krebs, H. A. (1979) *J. Biol. Chem.* **254**, 6538–6547.
9. Bailes, D. R., Bryant, D. J., Bydder, G. M., Case, H. A., Collins, A. G., Cox, I. J., Harman, R. R., Hall, A. S., Khenia, S., McArthur, P., Ross, B. D. & Young, I. R. (1987) *J. Magn. Reson.* **74**, 158–170.
10. Blackledge, M. J., Hayes, D. J., Challiss, R. A. J. & Radda, G. K. (1986) *J. Magn. Reson.* **69**, 331–336.
11. Bottomley, P. A., Foster, T. H. & Leue, W. M. (1984) *Proc. Natl. Acad. Sci. USA* **81**, 6856–6860.
12. Brown, T. R., Kincaid, B. M. & Ugurbil, K. (1982) *Proc. Natl. Acad. Sci. USA* **79**, 3523–3526.
13. Challiss, R. A. J., Blackledge, M. J. & Radda, G. K. (1988) *Am. J. Physiol.* **254**, C417–C422.
14. Haase, A. & Frahm, J. (1985) *J. Magn. Reson.* **64**, 94–102.
15. Haase, A., Frahm, J., Hänicke, W. & Mathai, D. (1985) *Phys. Med. Biol.* **30**, 341–344.
16. Hall, L. D., Sukumar, S. & Talagala, S. L. (1984) *J. Magn. Reson.* **56**, 275–278.
17. Hall, L. D., Webb, A. G. & Williams, S. C. R. (1989) *J. Magn. Reson.* **81**, 565–569.
18. Haselgrove, J. C., Subramanian, V. H., Leigh, J. S., Gyulai, L. & Chance, B. (1983) *Science* **220**, 1170–1173.
19. Kumar, A., Welti, D. & Ernst, R. R. (1975) *J. Magn. Reson.* **18**, 69–83.
20. Maudsley, A. A., Hilal, S. K., Perman, W. H. & Simon, H. E. (1983) *J. Magn. Reson.* **51**, 147–152.
21. Pyckett, I. L. & Rosen, B. R. (1983) *Radiology* **149**, 197–201.
22. Forsen, S. & Hoffman, R. A. (1963) *J. Chem. Phys.* **39**, 2892–2901.
23. Brown, T. R., Ugurbil, K. & Shulman, R. G. (1977) *Proc. Natl. Acad. Sci. USA* **74**, 5551–5553.
24. Brindle, K. M. (1988) *Prog. Nucl. Magn. Reson. Spectrosc.* **20**, 257–293.
25. Alger, J. R. & Shulman, R. G. (1984) *Q. Rev. Biophys.* **17**, 83–124.
26. Hsieh, P. S. & Balaban, R. S. (1987) *J. Magn. Reson.* **74**, 574–579.
27. Nakada, T., Kwee, I., Card, P. J., Matwiyoff, N. A., Griffey, B. V. & Griffey, R. H. (1988) *Magn. Reson. Med.* **6**, 307–313.
28. Mora, B. N., Narasimhan, P. T., Ross, B. D. & Allman, J. M. (1991) *Magn. Reson. Med.*, in press.
29. Cadoux-Hudson, T. A., Blackledge, M. J. & Radda, G. K. (1989) *FASEB J.* **3**, 2660–2666.
30. Krebs, H. A. (1972) *Essays Biochem.* **8**, 1–34.